ELSEVIER

Journal of Biomechanics 41 (2008) 299–306

JOURNAL OF BIOMECHANICS

www.elsevier.com/locate/jbiomech
www.JBiomech.com

Functional muscle synergies constrain force production during postural tasks

J. Lucas McKay[a], Lena H. Ting[b,*]

[a]School of Electrical and Computer Engineering, Georgia Institute of Technology, Atlanta, GA, USA
[b]The Wallace H. Coulter Department of Biomedical Engineering at Georgia Tech and Emory University, 313 Ferst Drive, Atlanta, GA 30332-0535, USA

Accepted 15 September 2007

Abstract

We recently demonstrated that a set of five functional muscle synergies were sufficient to characterize both hindlimb muscle activity and active forces during automatic postural responses in cats standing at multiple postural configurations. This characterization depended critically upon the assumption that the endpoint force vector (synergy force vector) produced by the activation of each muscle synergy rotated with the limb axis as the hindlimb posture varied in the sagittal plane. Here, we used a detailed, 3D static model of the hindlimb to confirm that this assumption is biomechanically plausible: as we varied the model posture, simulated synergy force vectors rotated monotonically with the limb axis in the parasagittal plane ($r^2 = 0.94 \pm 0.08$). We then tested whether a neural strategy of using these five functional muscle synergies provides the same force-generating capability as controlling each of the 31 muscles individually. We compared feasible force sets (FFSs) from the model with and without a muscle synergy organization. FFS volumes were significantly reduced with the muscle synergy organization ($F = 1556.01$, $p \ll 0.01$), and as posture varied, the synergy-limited FFSs changed in shape, consistent with changes in experimentally measured active forces. In contrast, nominal FFS shapes were invariant with posture, reinforcing prior findings that postural forces cannot be predicted by hindlimb biomechanics alone. We propose that an internal model for postural force generation may coordinate functional muscle synergies that are invariant in intrinsic limb coordinates, and this reduced-dimension control scheme reduces the set of forces available for postural control.

Keywords: Musculoskeletal model; Muscle synergies; Endpoint force; Muscle noise; Feasible force set; Balance; Cat

1. Introduction

A common finding among studies of the neural control of movement is "dimensional collapse," whereby the behavior of neuromechanical systems that are in theory highly redundant (Bernstein, 1967) and computationally formidable to control can be described with only a few degrees of freedom (Flash and Hochner, 2005; Grasso et al., 1998; Sanger, 2000; Zatsiorsky et al., 2003). However, despite this apparent motor abundance, recent studies of muscle coordination have demonstrated that the superposition of a few muscle activation patterns, defined as muscle synergies, is sufficient to describe muscular activity during many natural behaviors in humans and animals (Cheung et al., 2005; Krishnamoorthy et al., 2003; Poppele and Bosco, 2003; Ting and Macpherson, 2005; Tresch et al., 1999).

The hierarchical structure suggested by these results has provided substantial new insight into the neural control of movement, however, comparably few studies have examined muscle synergies quantitatively from the perspective of biomechanical function (e.g., Loeb et al., 2000; Raasch and Zajac, 1999; Valero-Cuevas, 2006). Comparing muscle synergies across subjects or animals, for example, is difficult not only because of experimental limitations (e.g., electrode placement) but also because muscle synergies that appear distinct may be functionally equivalent due to biomechanical redundancy. Similarly, because the number of synergies cannot be controlled in experiments, estimating the number of synergies that are

*Corresponding author. Tel.: +1 404 894 5216; fax: +1 404 385 5044.
E-mail address: lting@emory.edu (L.H. Ting).

0021-9290/$ - see front matter © 2007 Elsevier Ltd. All rights reserved.
doi:10.1016/j.jbiomech.2007.09.012

sufficient for task performance is an open question, albeit an important one from the perspective of rehabilitation (Latash and Anson, 2006).

In a recent study (Torres-Oviedo et al., 2006), we demonstrated that electromyographic and kinetic data from automatic postural responses in cats could be simultaneously decomposed into a small set of five "functional" muscle synergies, which specify both a fixed pattern of hindlimb muscle activation (a muscle synergy) and a correlated "synergy force vector" at the ground. Variation in the muscle activation patterns and forces produced when the cats stood in different postural configuration (anterior–posterior "stance distances," Macpherson, 1994) could be accounted for by the same muscle synergies, if we assumed that the forces generated by each muscle synergy rotated with the limb axis as it varied in the sagittal plane. This result was compelling because it suggests that an internal model (Kawato, 1999; Shadmehr and Mussa-Ivaldi, 1994) for limb force production during postural control coordinates synergy force vectors that are invariant in the intrinsic coordinates of the limb, although the postural task itself—generating an appropriate net response force at the ground with all four limbs—is based in extrinsic coordinates.

The first aim of the present work was to verify whether the rotation of synergy force vectors implicit in our analysis of the experimental data was feasible in the context of a detailed musculoskeletal model of the cat hindlimb (Burkholder and Nichols, 2004; McKay et al., 2007). While our prior analysis demonstrated that the measured EMG and force components could be correlated via the assumed muscle synergy to endpoint force transformation, we could not demonstrate that this relationship was biomechanically causal. In this study, synergy force vectors identified in the control posture of each animal from the previous work (Torres-Oviedo et al., 2006) were used as source data, and simulated muscle synergies corresponding to each hypothesized synergy force vector were determined with numerical optimization (e.g., van Bolhuis and Gielen, 1999; Crowninshield and Brand, 1981; Harris and Wolpert, 1998; Kurtzer et al., 2006; Valero-Cuevas et al., 1998). We then applied these muscle synergies to the model in other postures to test whether the resulting force vectors were oriented consistently with respect to the limb axis.

The second aim of the present work was to assess the impact of a muscle synergy organization on the functional capabilities of the hindlimb during postural control. We tested the hypothesis that constraining the muscles in the model to be activated by a few muscle synergies would limit the model's total force-production capacity. We quantified the force-production capacity of the model using feasible force sets (FFSs; Valero-Cuevas et al., 1998). Each FFS is a convex manifold in three-dimensional "force space"; the length of the vector from the origin to any point on the FFS represents the maximum force that can generated by the model in that direction, subject to limits on individual muscle forces. The FFS is a useful descriptor because neural deficits reduce its volume and influence its shape (Kuxhaus et al., 2005). We computed FFSs across postures assuming: (1) control of individuated muscles, limited only by each muscle's maximum force (nominal FFS), and (2) control only of the simulated muscle synergies (synergy-limited FFS). We then compared the FFSs from the two conditions (cf. Valero-Cuevas, 2006) to identify systematic changes; a reduction in FFS volume associated with the synergy constraint, for example, indicates that the synergy organization limits the overall force-production capacity, similar to a neuromuscular deficit. Finally, we investigated whether the stereotyped, posture-dependent changes observed in postural force production (the "force constraint strategy," Macpherson, 1994) were predicted by posture-dependent changes in the nominal or synergy-limited FFS shape.

2. Methods

We used a static musculoskeletal model of the cat hindlimb (McKay et al., 2007) and kinematic and kinetic data of three cats performing a horizontal translation balance task at four (cats *Bi* and *Ru*) or three (cat *Ni*) postural configurations to simulate functional muscle synergies based on those of Torres-Oviedo et al. (2006). Model postures approximating the average background period kinematics of each animal in each postural configuration (11 in total) were calculated as in McKay et al. (2007). Due to practical limitations (cf. Lloyd and Besier, 2003) we could not use previously reported muscle synergies directly (see Appendix A). Therefore, muscle activation patterns that could produce each of the five synergy force vectors reported from the control ("preferred") posture in each animal were determined using two optimization criteria drawn from the literature: "minimum-noise" optimization and "maximum-force" optimization.

We examined the endpoint force vectors of these simulated muscle synergies as hindlimb postural configuration varied to test the assumption (Torres-Oviedo et al., 2006) that changes in these vectors would be confined primarily to rotation in the sagittal plane. With this tested, we conducted an FFS analysis to assess whether a muscle synergy organization based on our simulated synergies would impact the force-production capability of the model by reducing FFS volume. A total of three FFSs were calculated for each of the 11 animal/posture combinations; first assuming individuated control of muscles (nominal FFS), then assuming only individuated control of the simulated synergies from the minimum-noise optimization (minimum-noise synergy-limited FFS), and last, assuming only control of the simulated synergies from the maximum-force optimization (maximum-force synergy-limited FFS). Finally, we compared the nominal and synergy-limited FFSs with experimental postural force data to determine whether the stereotyped, posture-dependent changes observed in postural forces were qualitatively predicted by posture-dependent changes in the FFSs. Statistical tests were considered significant at $p<0.05$ (Appendix B).

2.1. Hindlimb model

The three-dimensional hindlimb model is presented in detail in McKay et al. (2007). Briefly, the model is a matrix equation relating 31-element muscle excitation vectors $\vec{e}$ to the six-element force and moment system $\vec{F}$ produced at the endpoint, approximated as the metatarsal–phalangeal joint:

$$\vec{F} = (J(\vec{q})^{\mathrm{T}})^{+} R(\vec{q}) F_{\mathrm{O}} F_{\mathrm{AFL}}(\vec{q}) \vec{e}, \quad (1)$$

where the vector $\vec{q}$ is comprised of the model's seven rotational degrees of freedom at the hip, knee, and ankle; $(J(\vec{q})^{\mathrm{T}})^{+}$ is the pseudoinverse transpose of the geometric system Jacobian; $R(\vec{q})$ is the moment-arm matrix; F_{O} is the

diagonal matrix of maximal muscle forces; and $F_{AFL}(\vec{q})$ is the diagonal matrix of scaling factors based on active muscle force–length characteristics. Muscle moment arm values and fiber lengths were determined with SIMM software (Musculographics, Inc., Santa Rosa, CA).

2.2. Muscle synergies

In our muscle synergy analysis (Torres-Oviedo et al., 2006; Tresch et al., 1999), muscle excitation vectors $\vec{e}$ are produced by the linear combination of a few non-negative muscle synergies $\vec{w}_1$, $\vec{w}_2$, …, $\vec{w}_{NSYN}$, where the number of muscle synergies N_{SYN} is fewer than the number of muscles N_{MUS}. Each muscle synergy, $\vec{w}_i$, defines a fixed pattern of activation across multiple muscles. The contribution of each muscle synergy to any given postural response is scaled by an activation coefficient, c_i. Therefore, the nervous system is limited to producing only N_{SYN} patterns of muscle activation. However, each muscle can belong to multiple muscle synergies, and multiple muscle synergies can be active simultaneously, so the net pattern of muscle activation, $\vec{e}$, is the sum of activations due to each synergy. In matrix form, this relationship is:

$$\vec{e} = W\vec{c}, \tag{2}$$

where $\vec{w}_1$, $\vec{w}_2$, …, $\vec{w}_{NSYN}$ are the columns of W and $\vec{c}$ is a vector of synergy activation coefficients. Combining Eqs. (1) and (2) yields an expression for the force and moment system $\vec{F}_c$ due to synergy activation $\vec{c}$:

$$\vec{F}_c = (J(\vec{q})^T)^+ R(\vec{q}) F_O F_{AFL}(\vec{q}) W\vec{c}. \tag{3}$$

Simulated muscle synergies based on experimentally measured synergy force vectors from the control posture of each cat were determined with two different linear optimization criteria—"minimum-noise" (Crowninshield and Brand, 1981; Harris and Wolpert, 1998; Kurtzer et al., 2006) and "maximum-force" (Valero-Cuevas et al., 1998) optimization (Appendix A).

2.3. Nominal and synergy-limited feasible force sets

Methods for constructing the nominal FFSs using individuated muscle control have been described in our previous work (McKay et al., 2007). Briefly, the muscle excitation $\vec{e}$ producing the largest possible force projection in each of 1000 directions distributed on the unit sphere were calculated using linear programming subject to the constraint that muscle activations varied between 0 and 1:

$$0 \leqslant e_j \leqslant, \quad j = 1, 2, \ldots, N_{MUS}. \tag{4}$$

The FFS was then defined as the smallest three-dimensional convex polygon that encompassed these 1000 force projections. It was determined using the *convhull* package in Matlab.

Synergy-limited FFSs were constructed using an analogous procedure. For each synergy-limited FFS, the synergy activation vector $\vec{c}$ producing the maximal biomechanically feasible force in each of 1000 directions distributed on the unit sphere was calculated using linear programming subject to the constraint (Eq. (4)) and the additional non-negativity constraint:

$$0 \leqslant c_k, \quad k = 1, 2, \ldots, N_{SYN}. \tag{5}$$

3. Results

Simulated synergy force vectors rotated monotonically with the limb axis in the sagittal plane as postural configuration varied, supporting the assumption implicit in the analysis of Torres-Oviedo et al. (2006) (Fig. 1). Synergy force vector angles were more highly correlated to limb axis angles in the sagittal plane ($r^2 = 0.94 \pm 0.08$, $\mu \pm \sigma$) than in the horizontal plane ($r^2 = 0.75 \pm 0.25$). The slopes of the regression lines were near unity in the sagittal plane (0.86 ± 0.44) and distributed about zero in the horizontal plane (0.28 ± 0.46); a slope of 1 would indicate that synergy force vectors were fixed in the reference frame of the limb axis.

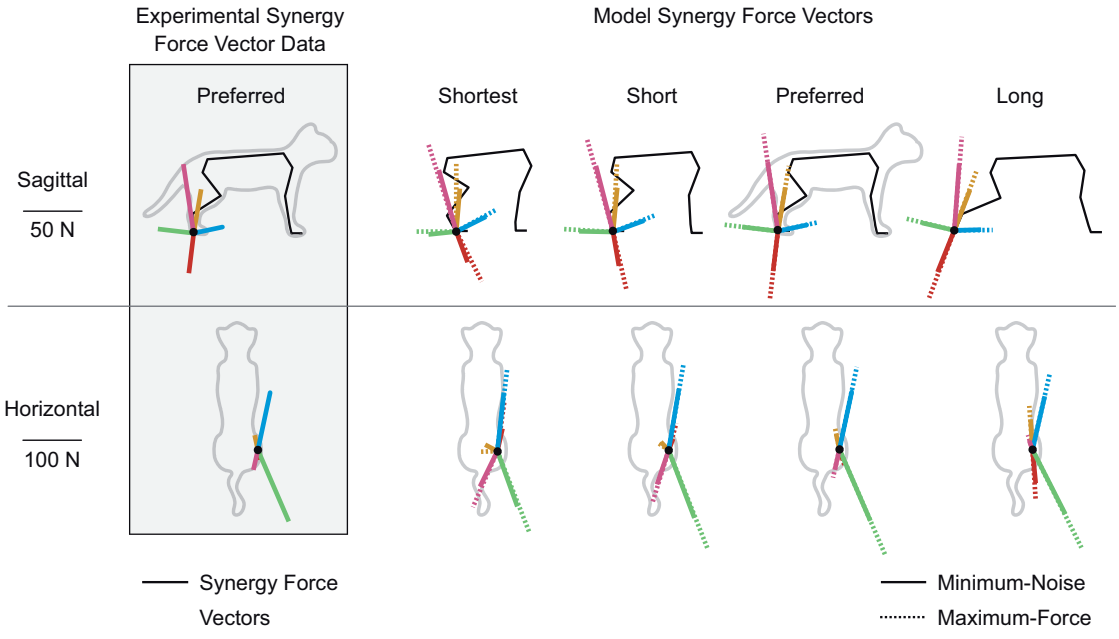

Fig. 1. Synergy force vector rotation with postural configuration. Left: Synergy force vectors from the control condition (preferred posture), as presented by Torres-Oviedo et al. (2006), used as source data. Average kinematics shown in black. Data shown are from cat *Ru*. Right: When simulated muscle synergies based on synergy force vectors at left are applied to the model in other postural configurations (shortest, short, long), the resulting synergy force vectors rotate monotonically with the sagittal-plane limb axis. Similar results are obtained whether minimum-noise (solid) and maximum-force (dashed) optimization is used to derive the simulated muscle synergies.

This monotonic rotation of synergy force vectors with the limb axis was independent of the optimization model used to derive the synergies. Minimum-noise and maximum-force synergy force vectors were aligned closely and differed primarily in magnitude, despite considerable differences in the muscle activation patterns from the two optimizations (Fig. 2). Large variations in muscle activity across animals have been previously demonstrated during both quiet standing and postural responses to perturbation even though the forces produced were similar (Fung and Macpherson, 1995; Torres-Oviedo et al., 2006).

Nominal FFSs (Fig. 3, gray polygons) were nearly isotropic in the sagittal plane, but anisotropic and oriented along the anterior–posterior axis in the horizontal plane (cf. McKay et al., 2007). Orientation of the nominal FFSs was not affected by changes in postural configuration; regression slopes were near zero in both sagittal (0.06 ± 0.25, $r^2 = 0.77 \pm 0.15$) and horizontal planes (0.01 ± 0.03, $r^2 = 0.60 \pm 0.50$).

Synergy-limited FFSs were qualitatively very different from the nominal FFSs (Figs. 3 and 4, white polygons) and were considerably more anisotropic in both the sagittal and horizontal planes, in particular with considerably reduced posterior force magnitude. From the standpoint of synergy-limited FFS shape, the only substantial difference between the two synergy optimization criteria was that FFSs based on maximum-force synergies encompassed some boundaries of the nominal FFSs, whereas minimum-noise FFSs did not. Synergy-limited FFSs rotated with the limb axis as posture varied, primarily in the sagittal plane (slope $= 1.41 \pm 2.32$, $r^2 = 0.92 \pm 0.05$ (sagittal); slope $= 0.33 \pm 0.17$, $r^2 = 0.75 \pm 0.14$ (horizontal)).

Changes in the synergy-limited FFS as posture varied (Fig. 4) were qualitatively similar to the changes in the distributions of active postural forces measured experimentally (Macpherson, 1994). In the sagittal plane, active forces and synergy-limited FFSs both rotated closely with the limb axis. In the horizontal plane, active forces and synergy-limited FFSs were elongated along a posterior diagonal axis at "long" posture and more widely distributed, with increased anterior force magnitude at "short" and "shortest" postures; these stereotypical changes have been described previously as the "force constraint strategy" (Macpherson, 1988).

Multiple ANOVA (Fig. 5) revealed that the synergy organization caused a highly significant reduction in FFS volume ($F = 1556.01$, $p \ll 0.005$). Tukey–Kramer pairwise comparisons applied post-hoc detected significant differences between the synergy-limited FFS volumes and nominal FFS volumes but no difference ($p > 0.05$) between the two optimization criteria. There was a significant main effect of stance distance ($F = 4.47$, $p < 0.012$); post-hoc tests revealed that FFS volume was highest in preferred posture. No effect of animal was detected ($F = 1.53$, $p > 0.22$). To increase statistical power, separate ANOVAs were performed to test the effect of posture on the three (nominal, minimum-noise, maximum-force) datasets; these results indicated significant effects of posture on the nominal FFS volumes ($F = 11.8$, $p < 0.004$) but not on the synergy-limited FFS volumes ($F = 0.31$, $p < 0.82$; $F = 0.25$, $p < 0.86$).

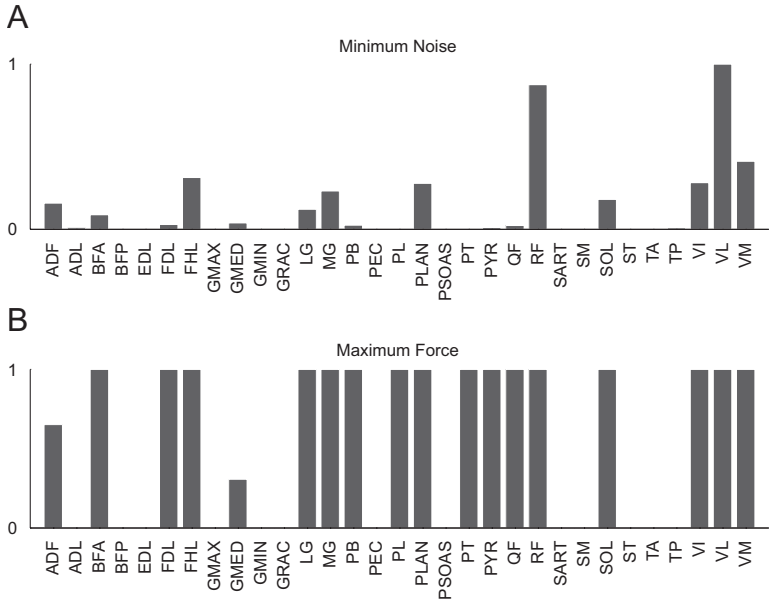

Fig. 2. Drastically different muscle synergies producing identically oriented synergy force vectors. The simulated muscle synergies shown were calculated to produce forces aligned with the synergy force vector shown in red for cat *Ru* in preferred posture (Fig. 1) using: (A) minimum-noise and (B) maximum-force optimization criteria. The minimum-noise optimization, equivalent to muscle stress minimization (Crowninshield and Brand, 1981), results in less coactivation than the maximum-force optimization.

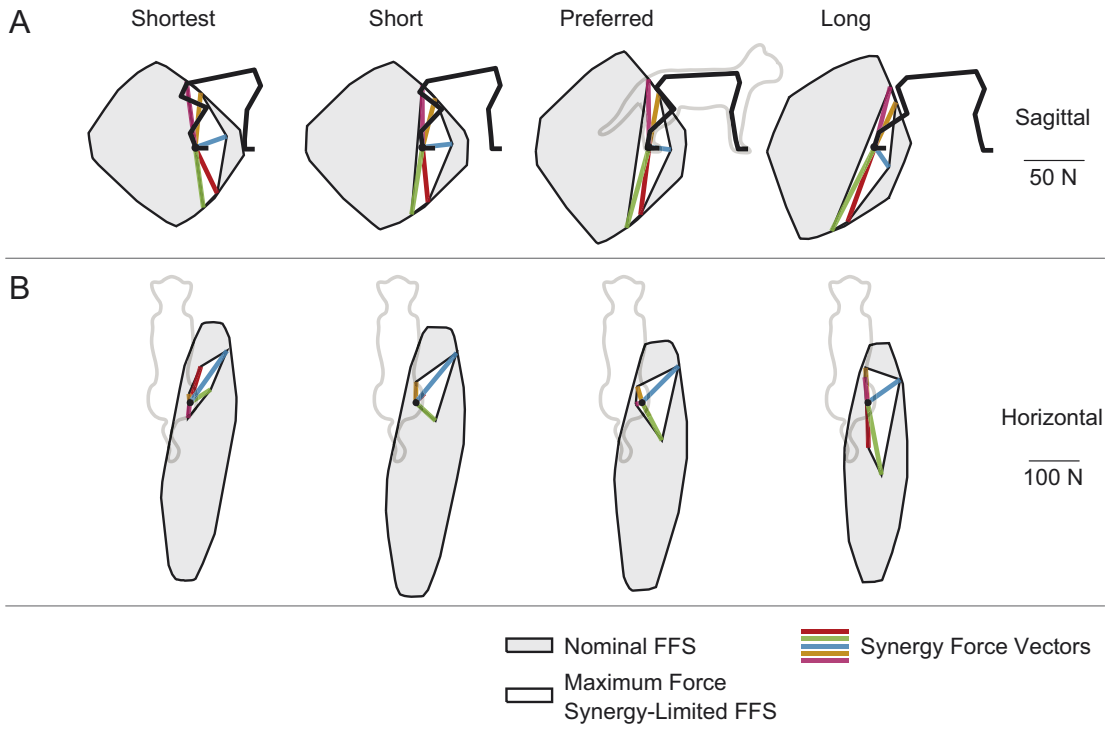

Fig. 3. Nominal FFS (gray), maximum-force synergy-limited FFS (white), and simulated maximum-force synergy force vectors (colored lines) for cat *Bi* in all postures: (A) sagittal projection and (B) horizontal projection. Enforcing the muscle synergy organization dramatically reduces the volume of the FFS in all postures. The synergy force vectors span the synergy-limited FFS, so that any point on the synergy-limited FFS can be reached with a linear combination of the synergy force vectors. While the nominal FFS is largely invariant across postures, the synergy-limited FFS rotates with the hindlimb axis in the sagittal plane, and changes shape acutely in the horizontal plane.

4. Discussion

The primary motivation of this work was to demonstrate the feasibility of the functional muscle synergy architecture proposed in our previous, experimental study (Torres-Oviedo et al., 2006) in the context of a detailed biomechanical model. Here we show that simulated synergy force vectors rotate monotonically with the limb axis in the sagittal plane as posture varies (Fig. 1), which was a critical assumption of our prior functional muscle synergy analysis. This result is important because it suggests that muscle synergies can be coordinated throughout the workspace to perform functional tasks in extrinsic coordinates with a parsimonious internal model based on a polar coordinate transformation. In the case of balance control, the orientation of the gravitational vector remains fixed while the orientations of the synergy force vectors vary with postural configuration. This type of computation is documented in the nervous system; for example, a cascade of polar transformations occurs in the first stages of voluntary reaching (Flanders and Soechting, 1990). It is thought that the initial proprioceptive frame for the transformation—at the level of the dorsal spinocerebellar tract—is likely a polar scheme based on limb length and orientation (Bosco et al., 1996; Poppele et al., 2002). Mechanistically, this transformation does not have to be explicit, as a neural substrate capable of computation in different reference frames has been demonstrated (Avillac et al., 2005).

The second result of this work is that we demonstrate the muscle synergy organization comes at a "cost" in terms of the force-production capability of the limb. When the synergy architecture was imposed, it caused a dramatic reduction in FFS volume (Figs. 3–5). This indicates that large regions of the FFS are inaccessible with only the synergies recruited for postural control. Based on this result, we predict that tasks like locomotion will recruit additional synergies to reach the remainder of the FFS. Synergies that are "shared" among tasks and "specific" to particular tasks have been identified in other animal and human preparations (d'Avella and Bizzi, 2005; Krishnamoorthy et al., 2004). However, it is only by examining muscle synergies in a biomechanical context that we are able to compactly illustrate why this might be the case.

The considerable changes in both FFS volume and shape associated with the synergy organization also suggest that it may prove valuable to consider the implications of muscle synergies when using models to predict behaviors involving submaximal forces, as opposed to "maximal" tasks (e.g., Kargo et al., 2002; Kuo and Zajac, 1993; Raasch et al., 1997; Valero-Cuevas et al., 1998), where behavior is likely limited by biomechanics alone. The nominal FFS has been demonstrated as a good predictor of endpoint force in such tasks, for example for forces ranging

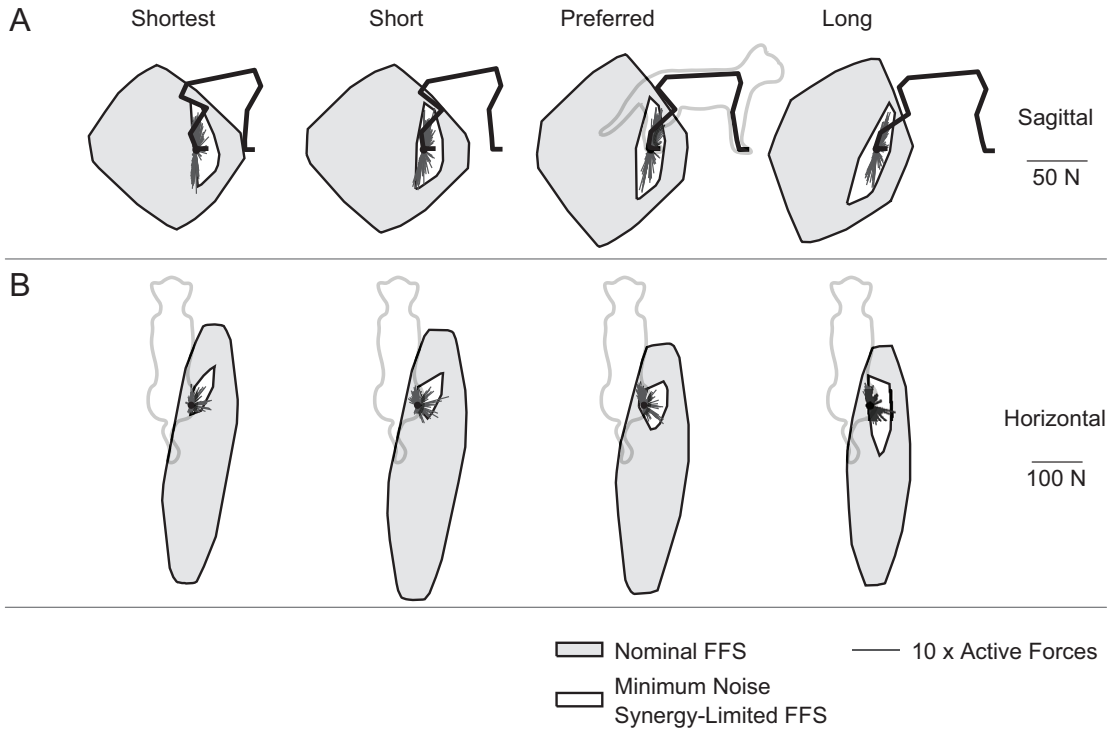

Fig. 4. Nominal FFS (gray), minimum-noise synergy-limited FFS (white), and active postural forces (dark gray, magnified 10 ×) for cat *Bi* in all postures: (A) sagittal projection and (B) horizontal projection. Active postural response forces are averaged across time windows as in Torres-Oviedo et al. (2006). The synergy-limited FFS is a substantially better predictor of the distribution of postural forces than the nominal FFS at all postures, particularly in the sagittal plane, where the synergy-limited FFS rotates closely with the envelope of postural forces. While the nominal FFS predicts almost no change in force production in the horizontal plane as posture varies, the synergy-limited FFS predicts stereotypical changes along a posterior diagonal axis (downwards and to the right, in the figure) at long posture and increased anterior forces (upwards, in the figure) at shortest posture, as is observed experimentally (Macpherson, 1994).

between 200 and 650 N in the human lower limb (Schmidt et al., 2003) and maximal forces in the finger (Valero-Cuevas et al., 1998). In contrast, we have previously demonstrated that the nominal FFS is a weak predictor of postural forces in preferred posture (McKay et al., 2007). Since postural forces are small (~1–2 and ~10 N in the horizontal and sagittal planes, respectively) compared to the biomechanical limits represented by the FFSs, the same endpoint forces vectors could have been used in all of the postural configurations, if the animals used individuated muscle control. Therefore, the changes in the postural forces are not necessitated by the biomechanics of the limb, but appear to arise due to a neural constraint on muscle coactivation in the form of the proposed muscle synergy organization. When we overlaid the experimental active postural response forces and the synergy-limited FFSs, we noted favorable agreement throughout the workspace (Fig. 4), suggesting that neural strategy of using the same muscle synergies across a range of postural configurations predominates the behavior.

These results were generally independent of the optimization criteria used to derive the synergies. While both optimization criteria used here predict behavior in some circumstances (Crowninshield and Brand, 1981; Kurtzer et al., 2006; Valero-Cuevas, 2000), the primary reason for selecting these particular criteria from the many models of their type that have been proposed (Crowninshield and Brand, 1981) was the drastically different solutions they produce (Fig. 2). Although the specific criterion that best predicts postural muscle activation patterns is unknown, we can hypothesize that any function lying between the extremes of penalizing muscle activation relatively drastically (“minimum-noise”) or not at all (“maximum-force”) would yield similar results. Experimentally, we observe similarities in synergy force vectors across individuals, yet marked differences in the muscle synergy patterns that are used consistently by each individual (e.g., d’Avella and Bizzi, 2005; Torres-Oviedo et al., 2006; Torres-Oviedo and Ting, 2007). These results corroborate the idea that the different muscle activation patterns across individuals may not necessarily indicate differences in force output.

Energetic optimality has historically been an elegant guiding principle in the study of movement (cf. Alexander, 1989; Hoyt and Taylor, 1981). When examining the motor hierarchy, both biomechanical and neural optimality principles may be simultaneously active. We noted that the volume of the nominal FFS, which reflects biomechanical limitations on force production, was significantly

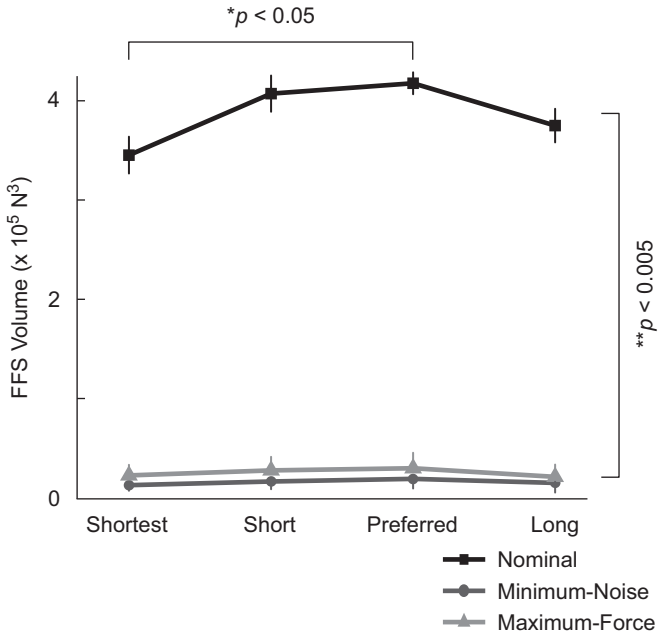

Fig. 5. Changes in nominal and synergy-limited FFS volume with posture. Data are presented as $\mu \pm \sigma$. Synergy-limited FFSs have significantly reduced volume (multiple ANOVA; $F = 1556.01$, $^{**}p \ll 0.005$) compared to nominal FFSs. Tukey–Kramer pairwise comparisons applied post-hoc detected significant differences between the synergy-limited FFS volumes and nominal FFS volumes but no difference between the two optimization criteria. There was a significant main effect of postural configuration ($F = 4.47$, $^{*}p < 0.012$); post-hoc tests revealed that FFS volumes in preferred posture were significantly higher than in shortest posture. No effect of animal was detected ($F = 1.53$, $p < 0.23$). To increase statistical power, separate ANOVAs were performed to test the effect of posture on the three (nominal, minimum-noise, maximum-force) datasets; these results indicated significant effects of postural configuration on the nominal FFS data ($F = 11.8$, $p < 0.004$) but not on the synergy-limited FFS data ($F = 0.31$, $p < 0.82$; $F = 0.25$, $p < 0.86$).

higher at the preferred posture (Fig. 5), consistent with the idea that the kinematics of this self-selected posture optimize this criterion. Similarly, Fung and Macpherson (1995) used an inverse dynamic analysis to demonstrate that the preferred posture kinematics minimize total joint torques for antigravity support. At other postures, the limb is levered at the girdle, preserving the intralimb geometry and locally minimizing joint torques. Similar kinematic invariance has been demonstrated repeatedly across species (Helms-Tillery et al., 1995; Sumbre et al., 2006). Therefore, we were surprised that the volume of the synergy-limited FFS, which reflects the combined biomechanical and neural limitations on force production for the task, did not vary significantly across postural configurations. These results suggest that synergy force vectors may be specifically selected among all possible force vectors to minimize posture-dependent changes in synergy-limited FFS volume. This is but one of the many possible "neural optimality" criteria that may work in concert with kinematic criteria; the contributions of both types of mechanisms should be considered to fully understand the neuromechanical coordination of the task.

Conflict of interest

The authors declare that they have no conflicts of interest.

Acknowledgments

The authors gratefully acknowledge Gelsy Torres-Oviedo for insightful discussions and providing synergy force vector data. Cat experimental data was courtesy of Jane Macpherson (NIH NS29025). Funding for this study was provided by NIH grant HD46922. The NIH had no role in the design, performance, or interpretation of the study.

Appendix. Supplementary material

Supplementary data associated with this article can be found in the online version at doi:10.1016/j.jbiomech.2007.09.012.

References

Alexander, R.M., 1989. Optimization and gaits in the locomotion of vertebrates. Physiological Reviews 69, 1199–1227.
Avillac, M., Deneve, S., Olivier, E., Pouget, A., Duhamel, J.R., 2005. Reference frames for representing visual and tactile locations in parietal cortex. Nature Neuroscience 8, 941–949.
Bernstein, N., 1967. The Coordination and Regulation of Movements. Pergamon Press, New York.
Bosco, G., Rankin, A.M., Poppele, R.E., 1996. Representation of passive hindlimb postures in cat spinocerebellar activity. Journal of Neurophysiology 76, 715–726.
Burkholder, T.J., Nichols, T.R., 2004. Three-dimensional model of the feline hindlimb. Journal of Morphology 261, 118–129.
Cheung, V.C.K., d'Avella, A., Tresch, M.C., Bizzi, E., 2005. Central and sensory contributions to the activation and organization of muscle synergies during natural motor behaviors. Journal of Neuroscience 25, 6419–6434.
Crowninshield, R.D., Brand, R.A., 1981. A physiologically based criterion of muscle force prediction in locomotion. Journal of Biomechanics 14, 793–801.
d'Avella, A., Bizzi, E., 2005. Shared and specific muscle synergies in natural motor behaviors. Proceedings of the National Academy of Sciences of the United States of America 102, 3076–3081.
Flanders, M., Soechting, J.F., 1990. Parcellation of sensorimotor transformations for arm movements. Journal of Neuroscience 10, 2420–2427.
Flash, T., Hochner, B., 2005. Motor primitives in vertebrates and invertebrates. Current Opinion in Neurobiology 15, 660–666.
Fung, J., Macpherson, J.M., 1995. Determinants of postural orientation in quadrupedal stance. Journal of Neuroscience 15, 1121–1131.
Grasso, R., Bianchi, L., Lacquaniti, F., 1998. Motor patterns for human gait: backward versus forward locomotion. Journal of Neurophysiology 80, 1868–1885.
Harris, C.M., Wolpert, D.M., 1998. Signal-dependent noise determines motor planning. Nature 394, 780–784.
Helms-Tillery, S.I., Ebner, T.J., Soechting, J.F., 1995. Task dependence of primate arm postures. Experimental Brain Research V104, 1–11.
Hoyt, D.F., Taylor, C.R., 1981. Gait and the energetics of locomotion in horses. Nature 292, 239–240.
Kargo, W.J., Nelson, F., Rome, L.C., 2002. Jumping in frogs: assessing the design of the skeletal system by anatomically realistic modeling and

forward dynamic simulation. Journal of Experimental Biology 205, 1683–1702.

Kawato, M., 1999. Internal models for motor control and trajectory planning. Current Opinion in Neurobiology 9, 718–727.

Krishnamoorthy, V., Goodman, S., Zatsiorsky, V., Latash, M.L., 2003. Muscle synergies during shifts of the center of pressure by standing persons: identification of muscle modes. Biological Cybernetics 89, 152–161.

Krishnamoorthy, V., Latash, M.L., Scholz, J.P., Zatsiorsky, V.M., 2004. Muscle modes during shifts of the center of pressure by standing persons: effect of instability and additional support. Experimental Brain Research 157, 18–31.

Kuo, A.D., Zajac, F.E., 1993. A biomechanical analysis of muscle strength as a limiting factor in standing posture. Journal of Biomechanics 26 (Suppl 1), 137–150.

Kurtzer, I., Pruszynski, J.A., Herter, T.M., Scott, S.H., 2006. Primate upper limb muscles exhibit activity patterns that differ from their anatomical action during a postural task. Journal of Neurophysiology 95, 493–504.

Kuxhaus, L., Roach, S.S., Valero-Cuevas, F.J., 2005. Quantifying deficits in the 3d force capabilities of a digit caused by selective paralysis: application to the thumb with simulated low ulnar nerve palsy. Journal of Biomechanics 38, 725–736.

Latash, M.L., Anson, J.G., 2006. Synergies in health and disease: relations to adaptive changes in motor coordination. Physical Therapy 86, 1151–1160.

Lloyd, D.G., Besier, T.F., 2003. An emg-driven musculoskeletal model to estimate muscle forces and knee joint moments in vivo. Journal of Biomechanics 36, 765–776.

Loeb, E.P., Giszter, S.F., Saltiel, P., Bizzi, E., Mussa-Ivaldi, F.A., 2000. Output units of motor behavior: an experimental and modeling study. Journal of Cognitive Neuroscience 12, 78–97.

Macpherson, J.M., 1988. Strategies that simplify the control of quadrupedal stance. I. Forces at the ground. Journal of Neurophysiology 60, 204–217.

Macpherson, J.M., 1994. Changes in a postural strategy with inter-paw distance. Journal of Neurophysiology 71, 931–940.

McKay, J.L., Burkholder, T.J., Ting, L.H., 2007. Biomechanical capabilities influence postural control strategies in the cat hindlimb. Journal of Biomechanics 40, 2254–2260.

Poppele, R., Bosco, G., 2003. Sophisticated spinal contributions to motor control. Trends in Neurosciences 26, 269–276.

Poppele, R.E., Bosco, G., Rankin, A.M., 2002. Independent representations of limb axis length and orientation in spinocerebellar response components. Journal of Neurophysiology 87, 409–422.

Raasch, C.C., Zajac, F.E., 1999. Locomotor strategy for pedaling: muscle groups and biomechanical functions. Journal of Neurophysiology 82, 515–525.

Raasch, C.C., Zajac, F.E., Ma, B., Levine, W.S., 1997. Muscle coordination of maximum-speed pedaling. Journal of Biomechanics 30, 595–602.

Sanger, T.D., 2000. Human arm movements described by a low-dimensional superposition of principal components. Journal of Neuroscience 20, 1066–1072.

Schmidt, M.W., Lopez-Ortiz, C., Barrett, P.S., Rogers, L.M., Gruben, K.G., 2003. Foot force direction in an isometric pushing task: prediction by kinematic and musculoskeletal models. Experimental Brain Research 150, 245–254.

Shadmehr, R., Mussa-Ivaldi, F.A., 1994. Adaptive representation of dynamics during learning of a motor task. Journal of Neuroscience 14, 3208–3224.

Sumbre, G., Fiorito, G., Flash, T., Hochner, B., 2006. Octopuses use a human-like strategy to control precise point-to-point arm movements. Current Biology 16, 767–772.

Ting, L.H., Macpherson, J.M., 2005. A limited set of muscle synergies for force control during a postural task. Journal of Neurophysiology 93, 609–613.

Torres-Oviedo, G., Ting, L.H., 2007. Muscle synergies characterizing human postural responses. Journal of Neurophysiology.

Torres-Oviedo, G., Macpherson, J.M., Ting, L.H., 2006. Muscle synergy organization is robust across a variety of postural perturbations. Journal of Neurophysiology 96, 1530–1546.

Tresch, M.C., Saltiel, P., Bizzi, E., 1999. The construction of movement by the spinal cord. Nature Neuroscience 2, 162–167.

Valero-Cuevas, F.J., 2000. Predictive modulation of muscle coordination pattern magnitude scales fingertip force magnitude over the voluntary range. Journal of Neurophysiology 83, 1469–1479.

Valero-Cuevas, F.J., 2006. A mathematical approach to the mechanical capabilities of limbs and fingers. In: Progress in Motor Control V. State College, PA.

Valero-Cuevas, F.J., Zajac, F.E., Burgar, C.G., 1998. Large index-fingertip forces are produced by subject-independent patterns of muscle excitation. Journal of Biomechanics 31, 693–703.

van Bolhuis, B.M., Gielen, C.C., 1999. A comparison of models explaining muscle activation patterns for isometric contractions. Biological Cybernetics 81, 249–261.

Zatsiorsky, V.M., Gao, F., Latash, M.L., 2003. Prehension synergies: effects of object geometry and prescribed torques. Experimental Brain Research 148, 77–87.